Preprint
UCRL-JC-137797

High Energy Electrons, Positrons and Photonuclear Reactions in Petawatt Laser-Solid Experiments

T. E. Cowan, A. W. Hunt, J. Johnson, M. D. Perry, W. Fountain, S. Hatchett, M. H. Key, T. Kuehl, T. Parnell, D. M. Pennington, T. W. Phillips, M. Roth, Y. Yakahashi, S. C. Wilks

U.S. Department of Energy
Lawrence Livermore National Laboratory

This article was submitted to
Joint Institute for Fusion Theory, Livermore, CA., November 23-24, 1998

September 9, 1999

This work was performed under the auspices of the United States Department of Energy by the University of California, Lawrence Livermore National Laboratory under contract No. W-7405-Eng-48.

High Energy Electrons, Positrons and Photonuclear Reactions in Petawatt Laser-Solid Experiments

T.E. Cowan[1], A.W. Hunt[4], J. Johnson[5], M.D. Perry[1], W. Fountain[3], S. Hatchett[1], M.H. Key[1], T. Kuehl[6], T. Parnell[3], D.M. Pennington[1], T.W. Phillips[1], M. Roth[6], Y. Takahashi[2] and S.C. Wilks[1]

[1]*Lawrence Livermore National Laboratory, Livermore, CA 94550*
[2]*University of Alabama, Huntsville, AL 35899*
[3]*Marshall Space Flight Center, Huntsville, AL 35812*
[4]*Harvard University, Cambridge, MA 02138*
[5]*University Space Research Association, Huntsville, AL 35806*
[6]*Gesellschaft für Schwerionenforschung, Darmstadt, Germany*

Abstract. The Petawatt laser at LLNL has opened a new regime of high-energy laser-matter interactions in which the quiver motion of plasma electrons is fully relativistic with energies extending well above the threshold for nuclear processes. We have observed that, in addition to the large flux of several MeV electrons ponderomotively expelled from the ultra-intense laser focus, there is a high energy component of electrons extending to ~100 MeV, apparently from relativistic self-focusing and plasma acceleration in the underdense pre-formed plasma. The generation of hard bremsstrahlung cascade as these electrons traverse the solid target material, and the resulting photo-nuclear reactions, nuclear fission, and positron-electron pair production are described.

INTRODUCTION

With the advent of high power, chirped-pulse amplification laser systems at a variety of laboratories, it has now become possible to produce highly relativistic laser plasmas [1]. These offer the possibility of very short pulse, high-energy electron and secondary radiation sources for a variety of investigations beyond tests of the fast ignition concept for which these lasers were originally developed. The prospect for producing very high energy electrons, bremsstrahlung and subsequent nuclear reactions, and of producing relativistic pair plasmas has been discussed theoretically [2,3].

With the Petawatt Laser at Lawrence Livermore National Laboratory [4], the experimental observation of these effects has become possible for the first time. Developed primarily for ICF research [5], the Petawatt uses one arm of the NOVA Nd:glass laser chain to amplify a frequency-chirped pulse to kJ energies before

temporal compression to ~450 fs. The peak power is well in excess of 1000 TW, and the large aperture beam can be focused with an 80 cm diameter f/3 on-axis parabola to a <20 μm spot, with intensity exceeding 3×10^{20} W/cm^2. At these extreme intensities the electromagnetic fields at the laser focus are enormous (E > 10^{13} V/m, and B > 10^5 Tesla) and the motion of the electrons in the target plasma is fully relativistic. The cycle-averaged oscillation or "quiver" energy of the electrons,

$$\overline{E} = mc^2\left[1+2U_p/mc^2\right]^{1/2}, \qquad (1)$$

can exceed several MeV, where $U_p = 9.33\times10^{-14}\ I$ (W/cm^2) λ^2 (μm) is the non-relativistic ponderomotive potential. The resulting distribution of electron energies in the target is predicted to resemble a Maxwellian [6], with mean energy given by Eq. 1, and it extends far beyond the threshold for which nuclear effects become important. An adjustable pre-pulse, at 2 or 10 ns before the main pulse and with an amplitude tunable over 10^{-4} to 10^{-1} of the peak energy, is used to pre-form an underdense plasma on the face of a solid target. This provides a medium in which to relativistically self-focus the laser beam to higher intensity, to increase the ponderomotive energies, and to produce self-modulated wakefield acceleration of electrons to even higher energies [7-9]. The resulting bremsstrahlung cascade in the solid target produces high energy bremsstrahlung, positron-electron pairs, and photonuclear reactions in the target material. In this contribution we describe our first ultra-intense laser-solid experiments with the Petawatt, in which we observed 100 MeV electrons, photonuclear reactions, laser-assisted nuclear fission, and positron-electron pair creation in ultra-intense laser-solid interactions.

ELECTRON SPECTROSCOPY EXPERIMENTS

To characterize the entire electron energy range of interest, from few MeV ponderomotive electrons to several hundred MeV or GeV-scale plasma-accelerated electrons, we have fielded two types of compact, permanent magnet electron spectrometers [10-12] as shown in Fig. 1. The data presented in this paper were taken with the two "low-energy" spectrometers, covering the electron energy range of 0.2 to 100 MeV. These were mounted at 30° and 95° with respect to the laser beam incident on the target. Permanent magnets of neodymium-iron-boron are used to produce a field strength of 5.5 kG, over a 10 cm × 15 cm pole face dimension with a 3.8 cm gap. The electrons are recorded in nuclear emulsion track detectors, which are positioned in the gap of the magnet such that the electron angle of incidence is a constant value of 10° throughout the dispersion plane. The emulsions consist of two layers of 50 μm thick, fine-grained silver bromide suspension coated on the front and back surface of a 500 μm polystyrene strip. Microscopic examination of the developed emulsion strips allows clear identification of charged particle tracks and distinguishes electrons emitted from the target by virtue of the density of exposed grains along the track, the angle of incidence, and the transverse position along the emulsion strip (which must be within the image of the entrance aperture). A second emulsion strip in each spectrometer is oriented to detect positrons within the energy range of 0.2 to 40 MeV. Below about 2 MeV, however, both electrons and positrons undergo sufficient multiple scattering in the emulsion that the incidence angle and track

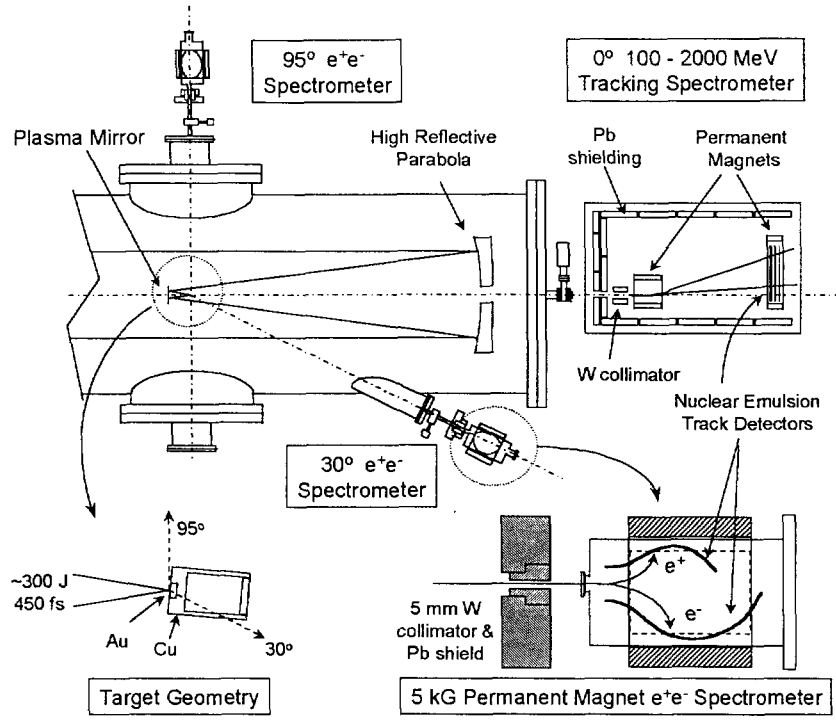

FIGURE 1. Schematic of the Petawatt target chamber and electron spectrometers. The compressed laser beam enters from the left, is reflected from the f=180 cm parabola to a secondary plasma mirror, and reflected onto the target at chamber center. The high-energy spectrometer (at right) measures electrons (~100 - 2000 MeV) emitted near 0°, which pass through a hole in the parabola. Low energy spectrometers measure electrons (0.2-140 MeV) and positrons (0.2-40 MeV) emitted at 30° and ~95° from the target (lower right).

length cannot be unambiguously determined and therefore cannot be distinguished from Compton electrons generated in the emulsions by the large flux of hard x-ray bremsstrahlung present in the solid target experiments. The spectrum of electron energies is obtained by counting the number of individual tracks in a specified microscopic field of view at several locations along the dispersion plane, and converting the track densities to absolute differential cross-sections. The energy dispersion (i.e., position versus energy) was calculated by ray-tracing and confirmed by calibration measurements performed at the LLNL 100 MeV electron Linac.

The first high energy electron spectra measured on the Petawatt are shown in Fig. 2, from an experiment in September 1997 to characterize the high-energy bremsstrahlung x-ray yield in short-pulse solid target interactions [13]. The target was a 0.5 mm thick × 2 mm diameter disk of gold, mounted in the end plate (~0.5 mm thick) of a cylindrical copper can (other targets shot in this geometry had thicker Au and Cu plates). As shown in Fig. 1, the laser light was focused using a secondary plasma mirror in a Cassegranian geometry. The total laser energy incident on the Au target was ~280 J, with a pulse duration of 450 fs. The energy

enclosed in the central focal spot was sufficient to achieve a focused intensity of $\sim 8\times10^{19}$ W/cm^2.

Two important features of these data are the large excess of 5-15 MeV electrons observed in the forward direction, and the presence of a very high energy tail extending to above 80 MeV in both spectra. The forward enhancement of the electron angular distribution is even larger than it appears because those electrons detected in the 30° spectrometer had to penetrate the target and in so doing lost substantial energy ($\Delta E \sim 2.5$ MeV for minimum ionizing particles) and were multiply scattered through rather large angles. Monte-Carlo electron transport calculations suggest that the forward electron flux between 2-15 MeV may be an order of magnitude or more larger than the factor of ~10 enhancement already apparent from Fig. 2. The low energy portion of the electron spectrum at both angles is also suppressed, compared to the actual energy distribution of electrons present in the target plasma, due to a large space charge potential (estimated to be several MV, roughly equal to U_p) which develops as electrons are expelled from the focus during the laser pulse. Because the laser pulse duration is so short, the return current of electrons flowing from the bulk of the target material does not have time to fully neutralize the positive space charge potential formed by the current of ejected relativistic electrons.

Including reasonable estimates of the above effects, the lower energy portion of these spectra, up to ~20 MeV, appear reasonably consistent with the expected Maxwellian distribution having a mean energy of ~3 MeV, predicted from Eq. 1, at the nominal intensity of $\sim 10^{20}$ W/cm^2. However, the presence of the high energy tail in each spectrum out to nearly 100 MeV, indicates a more complicated laser-target interaction [14]. The laser pre-pulse in this experiment is estimated to have pre-formed a ~50 μm scale-length plasma at the surface of the gold target,

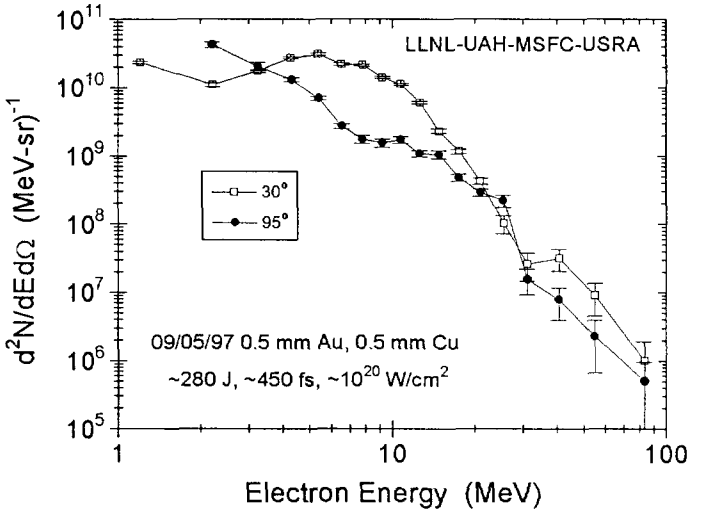

FIGURE 2. Distribution of electrons measured in magnetic spectrometers at 30° (open) and 95° (solid), from the first short-pulse (0.5 ps) Petawatt shot series on September 5, 1997. The 0.5 mm Au target was backed by 0.5 mm Cu. The estimated incident laser energy was 280 J, delivered in 450 ± 50 fs, with an estimated focused intensity of 8×10^{19} W/cm^2.

sufficient to cause either self-focusing of the laser light to much higher intensity, or self-modulated laser plasma acceleration.

LASER-DRIVEN PHOTO-NUCLEAR TRANSMUTATION

The presence of very energetic electrons in the forward directed spectrum in Fig. 2 suggests the generation of a substantial flux of hard bremsstrahlung x-rays produced by the passage of the relativistic electrons through the gold target. The portion of the bremsstrahlung spectrum above the threshold for photonuclear reactions should contribute to photoneutron emission from the gold and copper and, if sufficiently intense, produce measurable long-lived activities in the target. Immediately following each laser shot, the target assemblies were measured with a high resolution HPGe gamma-ray spectrometer to identify the specific daughter

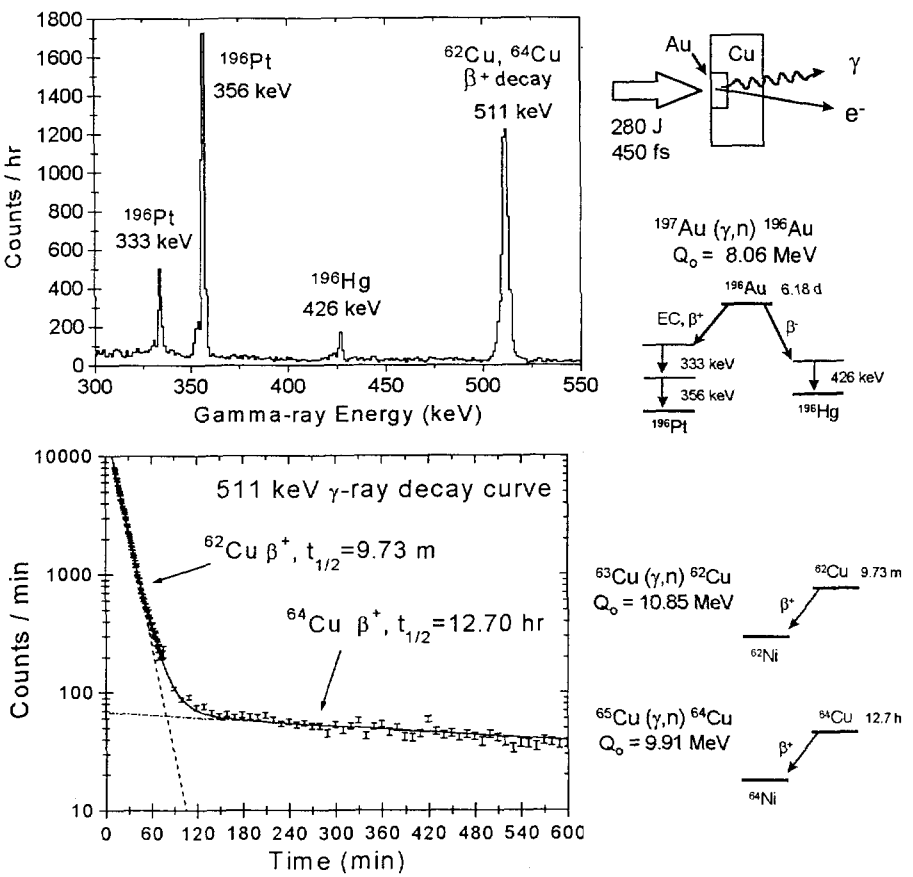

FIGURE 3. Photoneutron activation of Au and Cu target material in an intense Petawatt laser shot. (Upper Left) Gamma-ray energy spectrum measured with a high purity Ge detector. Peaks correspond to nuclear de-excitation gamma-rays following decay of ^{196}Au to ^{196}Pt and ^{196}Hg (see decay scheme at Right). (Lower Left) Count-rate vs. Time for the 511 keV gamma-ray peak from positron annihilation following β+ decay of ^{62,64}Cu to ^{62,64}Ni. Curves show two-component fit of exponential decay corresponding to the half-lives for the β+ decay of ^{62}Cu and ^{64}Cu.

nuclides present. A typical gamma-ray energy spectrum for an activated target is shown in Fig. 3. The production of ^{196}Au nuclei by ^{197}Au(γ,n)^{196}Au is clearly identified by the appearance of the nuclear de-excitation gamma-rays in the ^{196}Pt daughter nuclide at 356 keV and 333 keV. In addition, the less probable β^- decay of ^{196}Au to ^{196}Hg is also identified by the line at 426 keV. The intensities of the 333, 356 and 426 keV gamma-ray lines were observed to exhibit a decay rate consistent with the 6.18 day half-life of the ^{196}Au parent, confirming their identification.

The measurable yield of ^{197}Au(γ,n)^{196}Au reactions indicates a large flux of bremsstrahlung photons above the threshold energy for this reaction of Q_o=8.06 MeV. Photoneutron activation of the principal copper isotopes by the reactions ^{65}Cu(γ,n)^{64}Cu [Q_o=9.91 MeV], and ^{63}Cu(γ,n)^{62}Cu [Q_o=10.85 MeV] are also observed by the beta decay of their neutron deficient daughters to ^{64}Ni and ^{62}Ni respectively. These were identified in this experiment by the 511 keV positron-annihilation gamma-ray line, whose decay curve shown in Fig. 3 reveals two principal components whose decay constants match the 9.7 min and 12.7 hr half-lives of ^{62}Cu and ^{64}Cu, respectively. We have therefore identified three photo-neutron reactions in gold and copper produced from the laser-target interaction. We believe that their subsequent radioactive decays to isotopes of platinum, mercury and nickel represent the first observations of the transmutation of an element from a laser-produced plasma [10].

From the total activation yield of each nuclide, and using the known $\sigma_{\gamma,n}$ nuclear cross sections, one may estimate the total flux of bremsstrahlung photons above the threshold energy Q_o emitted into the forward hemisphere (i.e., intercepting the bulk of the target material) [10,15]. For example, the ^{63}Cu(γ,n)^{62}Cu activation yield implies a total forward-going flux of ~10^{11} photons above 10.85 MeV, for the data of Fig. 2.

LASER-DRIVEN NUCLEAR FISSION OF ^{238}U

In a subsequent experiment [16], we searched for laser-driven nuclear fission by performing a similar activation measurement with a small sample of ^{238}U placed in the Cu target holder (see Fig. 1). As shown in Fig. 4, the gamma-ray spectrum of target activations is considerably more complex than in the previous Au and Cu shots because of the large number of long-lived fission fragments. We used time-resolved gamma-ray spectroscopy to unambiguously identify the various fragments by both their characteristic gamma-ray energies and known half-lives [17]. The nuclides we have identified include ^{87,88}Kr, ^{92,93}Sr, ^{93,94,95}Y, ^{101,104}Tc, ^{105}Ru, ^{107}Rh, ^{128}Sb, ^{128}Sn, ^{134}Te, ^{135}I, ^{138}Xe, ^{138}Cs, ^{141}Ba and ^{146}Ce. The direct contribution to the yield of a given nuclide by the fission process was obtained from the total yield, after making corrections for contributions from other decay chains. We have compared our data to previous measurements [18] of these yields for specific nuclides from photofission of ^{238}U with accelerator-based bremsstrahlung beams. As shown in Fig. 3, the mass distribution of the fission products lie upon the usual double-humped distribution, which results from the large deformation of the ^{238}U parent. The fission yield at the peak of the mass distribution has been found empirically to be insensitive to the details of the initial ^{238}U excitation (e.g., whether photo- or neutron-capture induced). By normalizing to an empirical 6%

cumulative yield per fission [18] for the ^{135}I daughter, we estimate a total yield in this experiment of $(1.8\pm0.2)\times10^{7}$ photofission events, ^{238}U(γ,f).

Photofission and photoneutron reactions have different gamma-ray threshold energies, which can be used to provide spectral information regarding the energy distribution of bremsstrahlung photons produced by the plasma electrons, over the photon energy range of ~5 to 20 MeV. This is a particularly valuable technique because it covers the energy range characteristic of the radiation processes present in ultra-intense laser-plasma interactions. In this range simpler photon absorption techniques are insensitive because the photon energy is above the Compton minimum in the mass attenuation coefficient. The photoneutron (γ,n) threshold energy is characteristic of the neutron binding energy in the target nuclide (e.g., ~8 MeV in ^{197}Au, and ~10 MeV in Cu). Whereas the photofission threshold in ^{238}U(γ,f) is only 5 MeV because the process requires only a modest excitation to deform the ^{238}U nucleus into its fissioning transitional state [18]. Figure 5 demonstrates the good agreement the measured photo-neutron and photo-fission

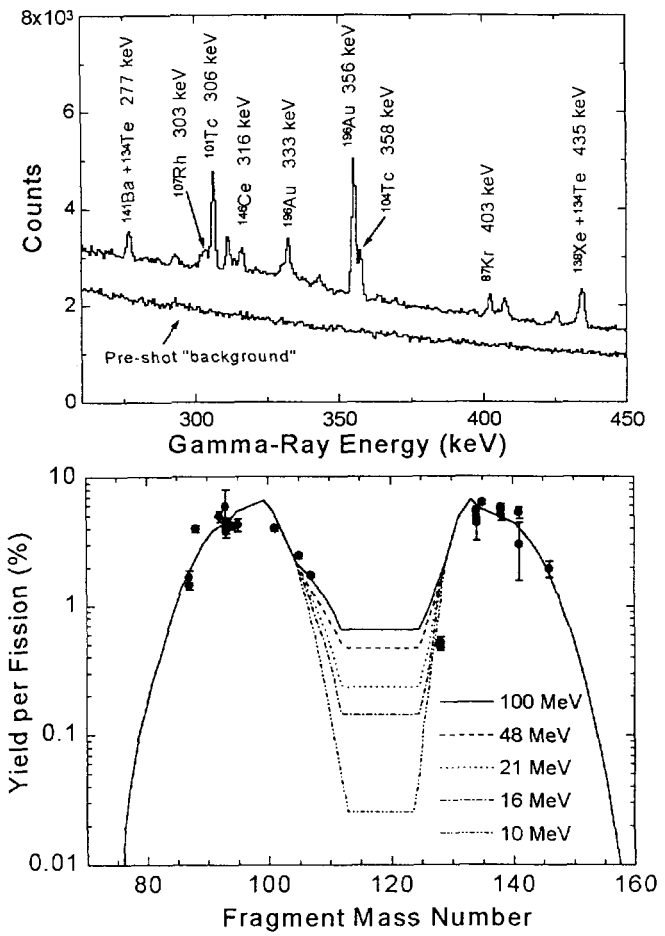

FIGURE 4. (Top) Energy distribution of γ-rays emitted from the Petawatt target assembly, measured before and after the laser shot (as marked). (Bottom) Mass distribution of fission fragments detected in this experiment.

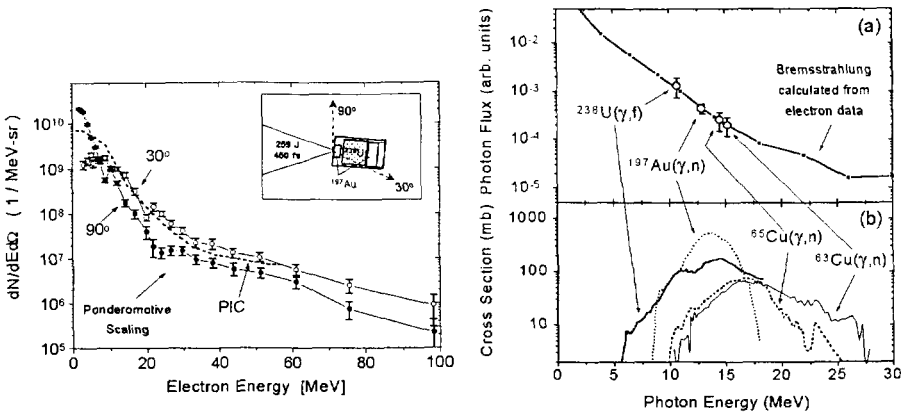

FIGURE 5. (Left) Measured electron distribution for fission shot. (Right) Comparison of photonuclear yields with calculated bremsstrahlung spectrum. Note that the exponential slope of the photon distribution emphasizes the importance of the near-threshold reaction cross-sections.

yields with that predicted from the bremsstrahlung distribution calculated from the measured electron spectrum.

POSITRON PRODUCTION

We have also been able to identify the production of positron-electron pairs in the ultra-intense laser-solid experiments on the Petawatt for the first time [11]. The yield of positron-electron pairs under our experimental conditions is expected to be of order 10^{-3} of the electron yield observed at 30°, in the energy range 5-10 MeV. The nuclear emulsion track detection technique is ideally suited for detection of such rare events, both because of its intrinsic single-particle detection sensitivity, and because of the relative immunity of emulsions to the intense high-energy x-ray flux generated in relativistic laser interactions at and above the critical plasma density. As noted above, the electron energy spectra are derived from spot inspection of the electron track density in the exposed emulsion, at several points along the dispersion plane. The typical electron track density at 10 MeV was of order 10^5 per cm^2, which corresponded to of order 10^2 tracks identified, under microscopic examination, within each 500 μm diameter field of view.

The sparse nature of the positron yield should provided for only of order ~1 track per microscopic field of view. Indeed, even in the first Petawatt 0.5 ps shot (Fig. 2), we observed single tracks consistent with the expected positron signature on the positron emulsion strip. However, to verify their identification, we have performed a complete scan of the entire emulsion strip, with critical attention paid to the quality and characteristics of each track to avoid spurious misidentification of scattered background events. This painstaking analysis was performed in a double-blind fashion, with the human scanners not informed of the total yield or spatial distribution of true positron signal tracks which was to be expected in this exposure. Similarly, the calculations of background processes have been performed without knowledge of the observed yield and distribution of tracks.

Satisfying three criteria identifies the positron candidates – the track grain density, the incident angle, and the transverse position of the track with respect to the dispersion plane. As scattered high energy electrons would also have the same grain density as the minimum-ionizing positrons, the spatial and angle distributions are of key importance in distinguishing between positrons emitted from the target and background scatter. To obtain the purest positron sample, we also required track identification from the front to back emulsion layers which, due to the large probability for multiple scattering in the intervening 500 μm of polystyrene, reduced the expected positron yield to largely unscattered events – a selection of only 5 to 10% of the total yield. The entrance angle distribution is determined from the projected track length on an event-by-event basis. The spatial distribution within the emulsion detector strip was the decisive information required to assess signal versus background rates. As shown in Fig. 6, we found that most events fell within the projected image of the entrance aperture along the detector plane. Of the 103 candidate events, we independently estimated that <3 were due to external conversion backgrounds in the spectrometer material, and estimated a signal between 50 and 200 events, based on preliminary estimates of the bremsstrahlung photon distribution in the target material. A full Monte Carlo calculation of the positron transport through the emulsions, and detailed

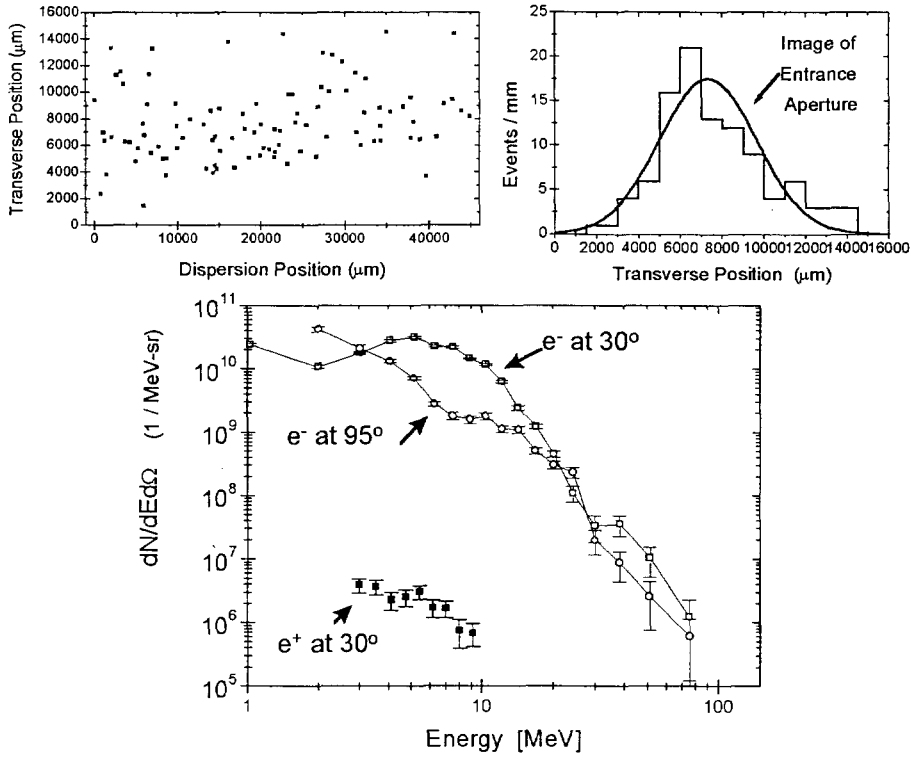

FIGURE 6. (Top Left) Distribution of positron tracks in emulsion detector plane, measured in the 30° spectrometer on the shot of Fig. 2. (Top Right) Histogram of track positions transverse to the dispersion plane, consistent with the projected image of the entrance aperture. (Bottom) Energy distribution of positrons measured between 3 and 9 compared to electron spectra from the same shot (see Fig. 2).

information of the bremsstrahlung shower in the target is required to make a quantitative comparison. Qualitatively, however, the measured events are consistent with the general energy spectrum expected from external pair production of the bremsstrahlung shower through the target, and scattering through the emulsion plane.

Although positron production is not surprising, given the presence of high energy bremsstrahlung produced in these laser-solid experiments, this measurement does represent the first observation of the conversion of pure laser energy into antimatter. The E-144 experiment at SLAC [19] has previously observed positron-electron pair production from an ultrarelativistic electron beam interaction with a low energy, short pulse laser. Although much more interesting in terms of the fundamental Quantum Electrodynamics under investigation in that experiment, the source of energy for the materialization of the pair was an artifact of the Lorentz boost into the rest frame of the beam, and therefore was extracted primarily from the kinetic energy of the incident electrons. In this case, the energy source is the incident laser beam, and in a sense represents the conversion (albeit inefficient and indirect) of ~eV photons from the laser to ~MeV photons (bremsstrahlung), followed by energy-to-mass conversion as well as the previously described nuclear excitations and reactions.

We have made additional measurements of positron production using much higher pulse energies (up to 750 J) and from much thinner targets. Preliminary data from thin Au foil targets (25 μm and 125 μm) show similar yields as above, although the bremsstrahlung production should be somewhat reduced in proportion to the target thickness. If this can be confirmed by continuing analyses presently in progress, it raises the exciting possibility that we may be observing pair production from the electron-ion collisions in the relativistic plasma, predicted by [3]. This would represent the first creation of a pair plasma in a laboratory experiment, albeit in the diffuse limit where the pair density is much smaller than the ion density. (Relativistic plasmas in which the pair density exceeds the ion density are thought be important in the accretion disks around black holes, and to play a role in the photon opacity in cosmological gamma-ray bursts.)

NARROW "JET" FEATURES

The eventual usefulness of ultra-intense laser plasma interactions for various fundamental or applied research, for example as single-stage particle accelerators and intense radiation sources, requires some degree of control and reproducibility. In the initial Petawatt experiments (e.g., Fig. 2), we observed a rather large variability in the shot-to-shot yields of electrons and hard bremsstrahlung. Subsequent experiments revealed the presence of intense beamed "jets" of electrons, similar to the directional emission now observed in a large variety of laser plasma experiments (e.g., see [20]). Very impressive examples from recent Petawatt experiments can be found in the overview by Key *et al.* [21]. In all of these experiments, however, the energy distribution of the electrons in the "jet" resembled a broad exponential, similar to the data of Fig. 2 [22-24]. On several Petawatt shots, however, we have observed electron "jets" of a different character in which the energy distribution is quite narrow, of order 20%. Two of these are shown in Fig. 7. Because we measure the electron energy distribution only within

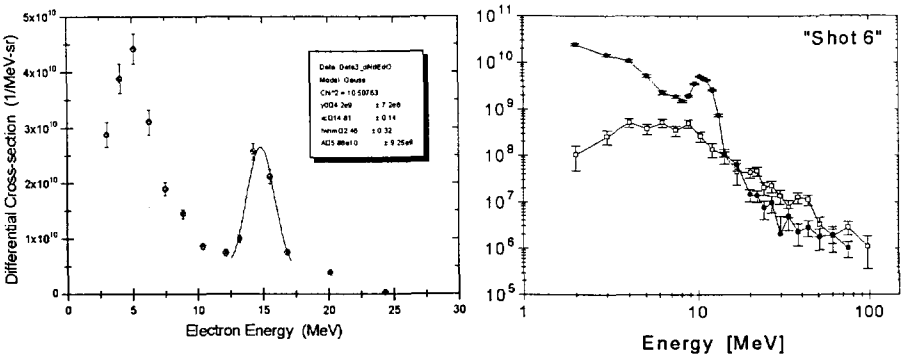

FIGURE 7. (Left) Electrons measured in the forward direction for 5 ps incident on 100 μm CH target. Note well-defined "jet" at ~15 MeV. (Right) Electrons measured transverse to incident laser pulse for 0.5 ps Petawatt pulse incident on 2 mm Au target. Note well-defined "jet" at 10.75 MeV.

a very small solid-angle, we do not have a direct measure of the angular spread of these monoenergetic features. However, using a detector of interleaved radiochromic film and Ta absorbers, we have observed evidence with very limited energy resolution for narrow beams which are consistent with a single electron energy and inconsistent with a broad exponential energy distribution. Whether these represent the high energy limit of the multi-photon ionization/ponderomotive acceleration beams observed at lower energy [25,26], or perhaps the first observation of monoenergetic laser acceleration is at present unknown. However if the production mechanism can be identified and controlled, it offers very exciting possibilities to use relativistic laser-plasma interactions for energetic particle generation.

SUMMARY

In summary, we have begun to explore a new regime of laser-matter interactions where the electron quiver energies are well above the threshold for causing nuclear reactions. We have observed a high energy component in the electron spectrum, up to ~100 MeV, in addition to a forward-directed lower-energy distribution which appears to be consistent with the relativistic dynamics of the electrons in the laser focus at the nominal focused intensities of $\sim 10^{20}$ W/cm^2. High energy bremsstrahlung produced in the gold targets was observed to produce photoneutron reactions in the gold target and copper sample-holder material. Photofission measurements of ^{238}U combined with the photoneutron data provide a powerful technique to characterize the high energy radiation produced in the bremsstrahlung cascade. Positron production has been observed, and further analysis will determine if it is due solely from the bremsstrahlung cascade or if, for the first time, we have observed pair production from a relativistic plasma. Finally, uncontrolled beams of electrons with narrow energy spread appear to accompany the very complex laser-matter interactions in the Petawatt solid-target experiments, which should motivate further interest in experimental study of this new high energy regime of relativistic laser-plasma physics.

We would like to acknowledge valuable contributions by many of our collaborators on the Petawatt program (see Ref. 21), and the support of the Nova staff for their help in fielding of these experiments. In particular we would like to

acknowledge the dedication and expert assistance of C. Brown and W. Patterson in designing and carrying out these experiments. This work was performed under the auspices of the U.S. Department of Energy by the Lawrence Livermore National Laboratory under Contract W-7405-Eng-48.

REFERENCES

1. M.D. Perry and G. Mourou, Science **264**, 917 (1994).
2. J. Meyer-ter-Vehn *et al.*, Laser Part. Beam **17:4** (1999).
3. E. Liang, S.C. Wilks and M. Tabak, Phys. Rev. Lett. **81**, 4887 (1998).
4. M.D. Perry *et al.*, Opt. Lett. **24**, 160 (1999).
5. M.H. Key *et al.*, Phys. Plasmas **5**, 1966 (1998).
6. S.C. Wilks *et al.*, Phys. Rev. Lett. **69**, 1383 (1992).
7. A. Pukov and J. Meyer-ter-Vehn, Phys. Rev. Lett. **76**, 3975 (1996).
8. K-C Tzeng and W. Mori, Phys. Rev. Lett. **79**, 5258 (1997).
9. E. Esarey *et al.*, Phys. Rev. Lett. **80**, 5552, (1998).
10. T.E. Cowan *et al.*, in: *Lasers '97*, (STS Press, McLean Va, 1998,), pp. 882-889.
11. T.E. Cowan *et al.*, Laser Part. Beam **17:4** (1999).
12. T.E. Cowan *et al.*, in: *Advanced Accelerator Concepts VIII* (AIP Press, 1999).
13. M.D. Perry *et al.*, Rev. Sci. Instrum. **77**, 1213 (1999).
14. S.C. Wilks *et al.* (to be published).
15. T.W. Phillips *et al.*, Rev. Sci. Instrum. **77**, 1213 (1999).
16. T.E. Cowan, A.W. Hunt, T.W. Phillips *et al.* (sub. to Phys. Rev. Lett.).
17. A.W. Hunt, T.E. Cowan, M.D. Perry *et al.* (to be publshied).
18. S. Kahane and A. Wolf, Phys. Rev. **C32**, 1944 (1985); E. Jacobs *et al.*, Phys. Rev. **C19**, 422 (1979); and H. Thierens *et al.*, Phys. Rev. **C14**, 1058 (1976).
19. D.L. Burke *et al.*, Phys. Rev. Lett. **79**, 1626 (1997)
20. D. Umstadter *et al.*, Science **273**, 472 (1996).
21. M.H. Key, T.E. Cowan, B.A. Hammel, S.P. Hatchett, E.A. Henry, J.D. Kilkenny, J.A. Koch, A.B. Langdon, B.F. Lasinski, R.W. Lee, J.D. Moody, M.J. Moran, A.A. Offenberger, D.M. Pennington, M.D. Perry, T.W. Phillips, T.C. Sangster, M.S. Singh, M.A. Stoyer, M.T. Tabak, M.T. Sukamoto, K. Wharton, S.C. Wilks, "Progress in Fast Ignitor Research with the Nova Petawatt Laser Facility," to be published in *Phys. Plasmas* (1999).
22. A. Modena *et al.*, Nature **377**, 606 (1995).
23. G. Malka and J.L. Miquel, Phys. Rev. Lett. **77**, 75 (1996).
24. K.B. Wharton *et al.*, Phys. Rev. Lett. **81**, 822 (1998).
25. C.I. Moore, J.P. Knauer and D.D. Meyerhofer, Phys. Rev. Lett. **74**, 2439 (1995).
26. C.I. Moore *et al.*, Phys. Rev. Lett. **82**, 1688 (1999).